JACS
JOURNAL OF THE AMERICAN CHEMICAL SOCIETY

Article

pubs.acs.org/JACS

Mechanism of Amination of β-Keto Esters by Azadicarboxylates Catalyzed by an Axially Chiral Guanidine: Acyclic Keto Esters React through an *E* Enolate

Luis Simón*,† and Jonathan M. Goodman*,‡

†Chemical Engineering Department, Facultad de Ciencias Químicas, Plaza de los Caídos 1-5, Salamanca E37004, Spain

‡Unilever Centre for Molecular Informatics, Department of Chemistry, University of Cambridge, Lensfield Road, Cambridge CB2 1EW, U.K.

Supporting Information

ABSTRACT: The mechanism of the reaction between di-*tert*-butyl azadicarboxylate and 1,3-dicarbonyl compounds catalyzed by an axially chiral guanidine is investigated by density functional theory methods. The results show that the catalyst acts simultaneously as a Brønsted base and an acid catalyst, and the mechanism is similar to that of the related BINOP organocatalysts. Surprisingly, cyclic and acyclic β-keto esters yield opposite enantiomers; the calculations demonstrate that this is a consequence of the preferred enolate geometry in the transition structures. Literature evidence suggests that other organocatalytic reactions show similar behavior.

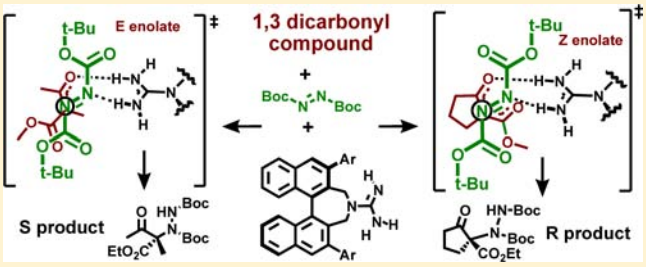

INTRODUCTION

The guanidine group is present and active in many interesting organocatalysts.[1−28] Mechanistic[29] and computational[30−35] studies have revealed that in many cases the guanidine group acts not only as a Brønsted base catalyst activating the nucleophile, but also as a proton donor catalyst to the reaction electrophile. On the other hand, phosphoric acid catalysts derived from 3,3′-substituted BINOL (BINOP) have been recognized as some of the most successful organocatalysts, with a broad range of applications in the nucleophilic additions to imines[36−41] and carbonyl groups.[42] Terada, who along with Akiyama[43] was a pioneer[44,45] in the development of BINOL-phosphoric acid catalysts, has also developed organocatalysts combining the 3,3′-substituted binaphthyl moiety present in the BINOP organocatalysts with a guanidine group in a nine-membered-ring structure[20−28] and a seven-membered-ring structure[26,46−49] (Figure 1).

We[50−53] and others[54−61] have found theoretical evidence that in BINOP organocatalysts the phosphoric acid moiety acts simultaneously as a proton acceptor with the nucleophile and a proton donor to the electrophile. This kind of double activation explains the high enantioselectivity observed according to a "three-point contact model", in which the catalyst establishes three simultaneous interactions with the transition states: two H-bonds with the nucleophile and the electrophile, and steric interactions with the large BINOP 3,3′ substituents. The presence of these three contacts is acknowledged as a requirement for chiral recognition.[62]

In this paper we investigate whether guanidine groups in Terada's seven-membered-ring axially chiral guanidine are also

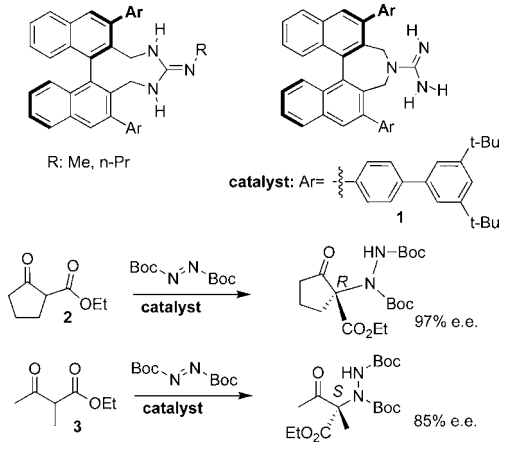

Figure 1. Nine-membered-ring[20−28] (top left) and seven-membered-ring[26,46−49] (top right) guanidine axially chiral catalysts developed by Terada. (Bottom) Stereochemistry of the amination of 1,3-dicarbonyl compounds catalyzed by *R* seven-membered-ring guanidine catalyst.

active by a proton-donor/proton-acceptor mechanism, and if the three-point contact model can also be applied to understand the enantioselectivity. These catalysts have been used in the amination of 1,3-dicarbonyl compounds[46] and α-cyanothioacetates[47] using di-*tert*-butyl azadicarboxylate, in the Henry reaction,[48] and in the [3+2] cycloadition of maleates to Schiff bases.[49] The study of the first of these reactions is particularly

Received: August 8, 2012
Published: September 11, 2012

   dx.doi.org/10.1021/ja307712y | J. Am. Chem. Soc. 2012, 134, 16869−16876

important since the sense of the enantioselectivity is reversed from cyclic to acyclic 1,3-dicarbonyl (Figure 1). An effective theoretical model should be able to explain this surprising experimental result.

COMPUTATIONAL METHODS

Calculations were performed using Gaussian09 program.[63] As in our previous studies on BINOP organocatalysts, we used ONIOM[64−66] QM/MM method in geometry optimizations and transition structure searches, combining UFF molecular mechanics method[67] in the low-level layer and B3LYP[68] density functional with 6-31G(d,p)[69−71] basis set in the high-level layer. The distribution of atoms in these two layers is shown below in Figures 3, 7, and 9, where atoms in the high-level layer are represented by a "ball-and-stick" model and atoms in the low-level layer are represented by a "wire" model. These figures were prepared using Pymol v.0.99 software. During transition-state searches, solvent (THF) was simulated by a polarizable continuum model (PCM)[72−76] using the cavity for the complete system defined by the UFF scheme (Gaussian09 default). Once a transition structure was obtained by this method, single-point energy was calculated using meta-GGA M06-2X functional,[77,78] adding diffuse functions[69] to heavy atoms to the 6-31G(d,p) basis set. We have demonstrated that the combination of B3LYP optimization and meta-GGA functionals affords reliable results with a reasonable computational effort.[79] During these single-point calculations, solvent was simulated with the PCM[72−76] and a UFF radius using the solvent-accessible surface for cavity generation. The single-point energy obtained was added to the zero-point energy correction calculated by the ONIOM (B3LYP/6-31G(d,p):UFF) method used for the optimization. Using this energy, relative populations corresponding to competing transition structures were calculated by mean of a Boltzmann distribution at 213 K (the temperature used in the experiments).

RESULTS AND DISCUSSION

We first investigated the reaction of cyclic β-keto ester **2** with di-*tert*-butyl azadicarboxylate catalyzed by chiral guanidine **1**. To save computational time, a methyl ester was used instead of the ethyl ester of the 1,3-dicarbonyl compound. Since Terada suggested in his paper that the enantioselectivity of the reaction could be explained on the basis of the ion-pair structures formed by the guanidinium catalyst and the enolate from 1,3-dicarbonyl substrate, we started calculating the transition states derived from them. We made an extensive search of structures: two relative orientations between nucleophile and electrophile and, for each, the four possible rotamers of the di-*tert*-butyl azadicarboxylate. For the resulting eight combinations, *R* and *S* transition structures were located. The results are summarized in Figure 2. In Figure 3, the two more stable transition structures leading to *R* and *S* product are shown.

The energies included for each structure are relative to the most stable transition state obtained for this reaction (*vide infra*). As shown in Figure 2, the guanidinium group interacts only with the 1,3-dicarbonyl enolate, although in some of the structures an additional weak H-bond exists between one of the guanidinium H-atoms and one of the di-*tert*-butyl azadicarboxylate oxygens. Therefore, these transition structures do not correspond to the above-mentioned three-point interaction model, in which the catalysts establishes two H-bond interactions with the transition state and a third interaction based on steric hindrance with its 3,3′ bulky groups. Instead, only one favorable interaction is present (between the guanidinium and the enolate), and the remaining two interactions required for chiral recognition are steric hindrance between the catalyst and the nucleophile and electrophile.

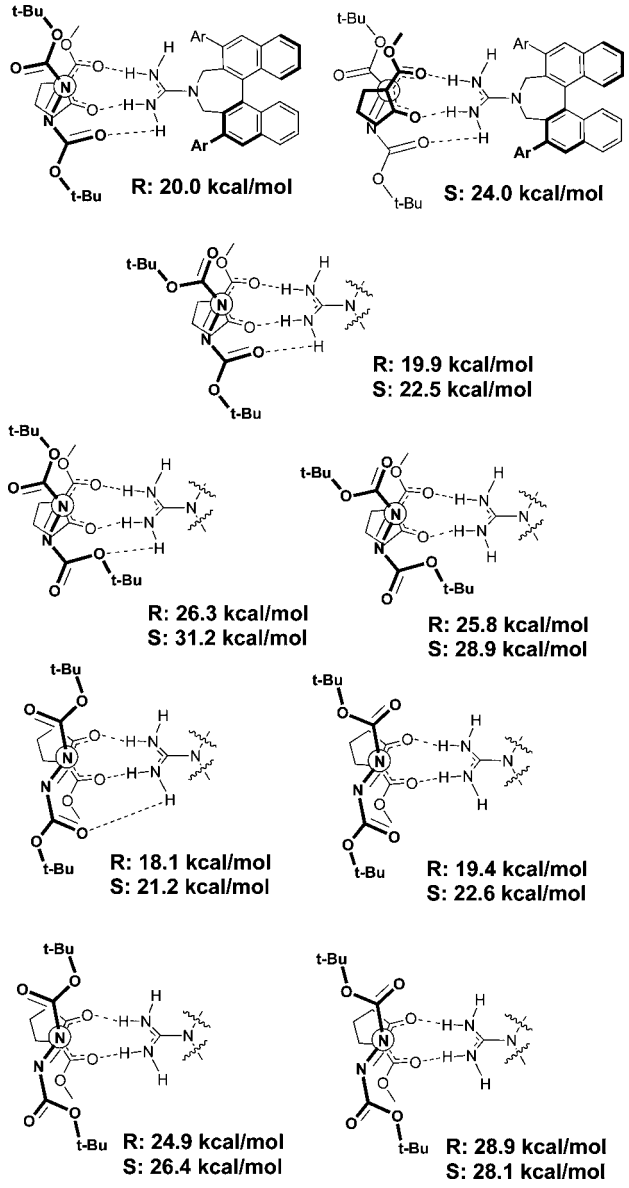

Figure 2. Transition structures for the addition of cyclic 1,3-dicarbonyl compound **2** to di-*tert*-butyl azadicarboxylate with the guanidinium doubly coordinated to the enolate. Note that *S* transition structure is only shown for the first electrophile conformation. Energies relative to the most stable transition state are expressed in kcal/mol.

The most stable transition state yields a product with absolute configuration *R*, and its zero-point energy difference with respect to the most stable *S* transition state (3.1 kcal/mol) would imply that the product would be obtained with an enantiomeric excess (ee) higher than 99.9%. Although numerical errors in the calculations may justify the difference with the experimental results (97% ee *R* product), the high energy of these transition structures makes it very unlikely that the reaction proceeds through this kind of mechanism. Therefore, we considered those possible transition structures in which the guanidine is H-bonded to the enolate and the electrophile.

As with previous mechanism, it is necessary to consider two possible relative orientations between the nucleophile and the electrophile (Figure 4a). This would correspond to *syn*/*anti* isomers in the reaction product, provided the stereochemistry in the tertiary N-atom generated could be maintained. Since

dx.doi.org/10.1021/ja307712y | J. Am. Chem. Soc. 2012, 134, 16869−16876

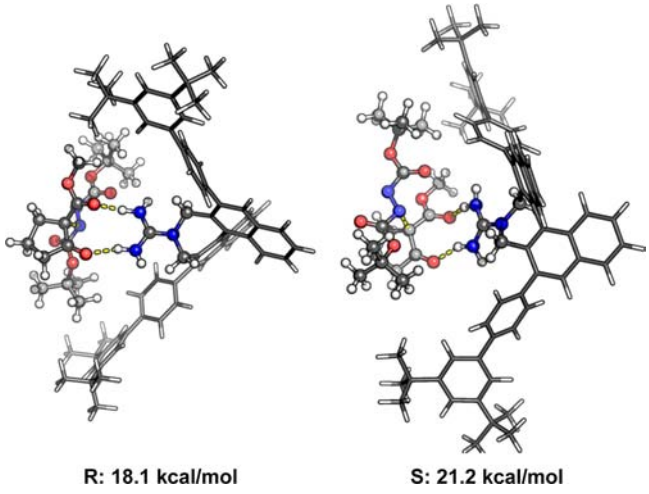

Figure 3. The two most stable transition structures, corresponding to the structure with the guanidinium doubly coordinated to the enolate mechanism.

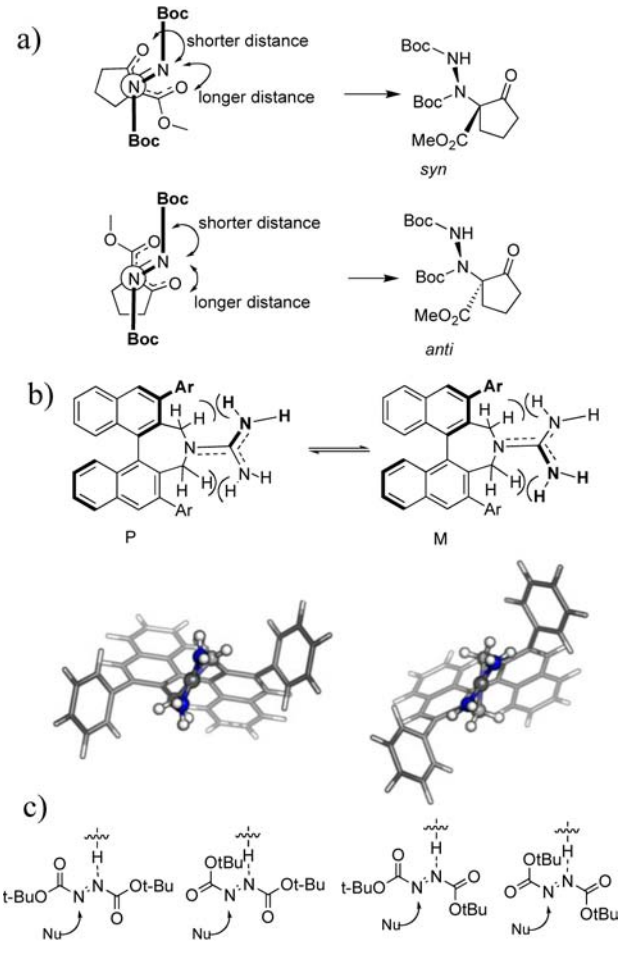

Figure 4. (a) *Syn* and *anti* relative stereochemistry in the reaction transition structures. Because the stereochemistry on the N-atom is not maintained in the products, it is not possible to isolate *syn* and *anti* products. (b) *P* and *M* helicity in guanidine catalyst axial conformers; note that, for clarity, only a phenyl group is shown in 3,3′ catalyst substituents. (c) Different conformations of di-*tert*-butyl azadicarboxylate.

this is not the case, it is not possible to find the diastereomeric ratio in the product, but we will refer to the corresponding transition structures using this nomenclature. In addition, we also observed that the guanidinium catalyst **1** can adopt two different conformations, since the two terminal N-atoms in the guanidine do not fit in the plane defined by the seven-membered-ring structure due to steric hindrance (Figure 4b). Observing these two conformers from the front, it is possible to see that they correspond to pseudoaxial chirality, and therefore they will be referred as *P* (plus) or *M* (minus) guanidine conformations in the transition structures. Our calculations reveal that the *P* conformer is 1.9 kcal/mol more stable than the *M* conformer. This energy difference is too small for us to neglect the presence of the *M* conformer in transition structures, and so both were considered in our calculations. Finally, the di-*tert*-butyl azadicarboxylate can also show different rotamers considering the *s-cis* or *s-trans* conformations around the C−N bonds (Figure 4c). Our previous calculations on Terada's mechanism (Figure 2) reveal that transition structures showing different electrophile conformers have small energy differences, and therefore the presence of any of these conformers cannot be discarded in any relevant transition structures.

The results for all possible combinations are shown in Figure 5, where the relative zero-point-corrected energies are referred to the most stable transition structure. Calculation of the populations of the products according to a Boltzmann distribution based on these energies yields an estimated 98% ee in favor of *R* product. This is in excellent agreement with the experimental results (97% ee for *R* product).

Analysis of the results shows a clear preference for *syn* over *anti* transition structures (the best *anti* transition state has a 3.4 kcal/mol higher energy than the best *syn* transition state). In *syn* transition structures, a shorter distance is observed between the ketone carbonyl O-atom and the H-bonded N-atom in the electrophile (around 2.7−2.8 Å) than between this N-atom and the ester carbonyl O-atom (around 3.7 Å). In *anti* transition structures, however, the distance between the N H-bond acceptor atom in the electrophile and the ester carbonyl is shorter than that with the ketone carbonyl. Considering the distance between the guanidine N-atoms (2.3 Å), H-bonding is geometrically favored with the ketone oxygen in *syn* and with the ester oxygen in *anti* transition structures. This could explain why *syn* transition structures show lower energies than *anti* ones, since the most stable tautomer corresponds to the ketone enolate form.[80] It also corresponds to the preference for *endo* over *exo* transition structures that we observed for the Friedel−Crafts reaction of indole with acyl imines.[52]

For *syn* transition structures leading to *R* product, the relative stability between *P* and *M* guanidine conformations depends on the rotamer of the di-*tert*-butyl azadicarboxylate present. In those cases in which the acyl group near the bulky catalyst substituent has *s-cis* conformation (Figure 6), the *M* guanidine conformation is preferred (0.9 vs 3.9 kcal/mol and 0.3 vs 6.5 kcal/mol); the steric hindrance between the *s-cis* Boc and the catalyst 3,3′ group is reduced in the transition state with the *M* conformation but not in the transition state with the *P* conformation. This is confirmed by single-point energy calculations of these structures in which the bulky catalyst substituent is replaced by a H-atom; in this case, the usual higher stability of *P* guanidine conformation is recovered. Accordingly, in those cases in which this acyl group has *s-trans* conformation, there is not an advantage in *M* guanidine structures, and the intrinsically more stable *P* guanidine conformation leads to more stable transition structures (0.0 vs 6.0 kcal/mol and 4.2 vs 6.0 kcal/mol).

dx.doi.org/10.1021/ja307712y | J. Am. Chem. Soc. 2012, 134, 16869−16876

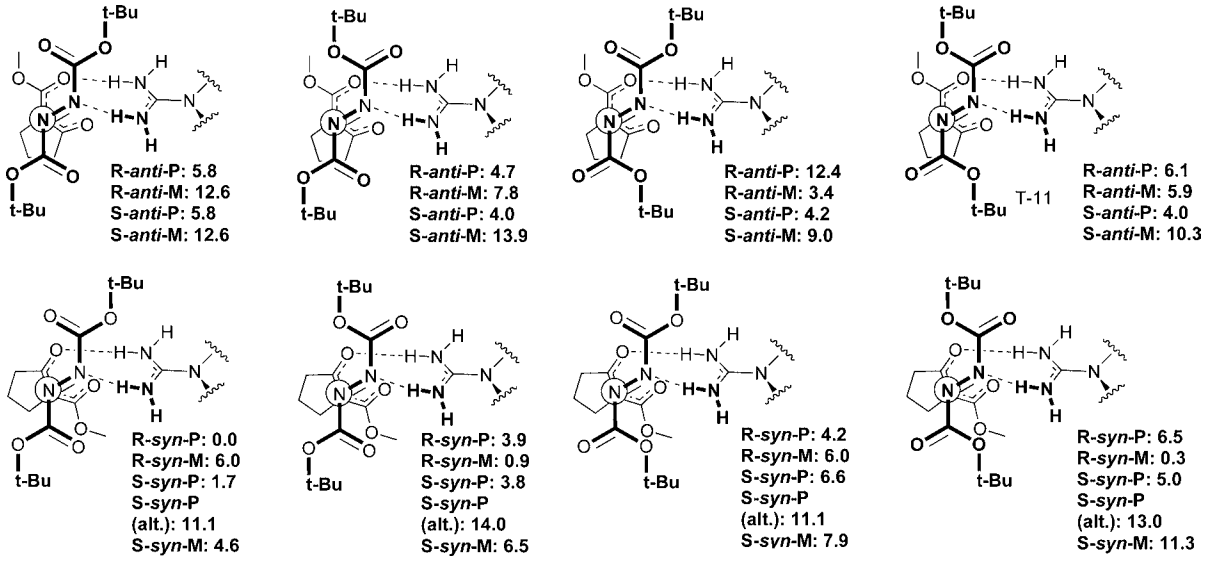

Figure 5. Transition structures for the addition of cyclic 1,3-dicarbonyl compound **2** to di-*tert*-butyl azadicarboxylate catalyzed by chiral guanidine **1** according to the mechanism in which the catalyst is bonded to the enolate and the electrophile. Note that only *S* transition structures are shown. In (alt.) transition structures, the H-bond is formed with the ester rather than the ketone O-atom (see text). Energies relative to the most stable transition state are expressed in kcal/mol.

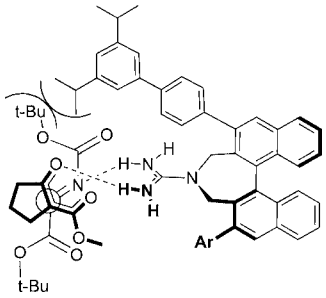

Figure 6. Steric hindrance that is reduced in the *M* guanidine conformation for *R-syn* transition structures. This effect is not observed when the acyl group has *s-trans* conformation.

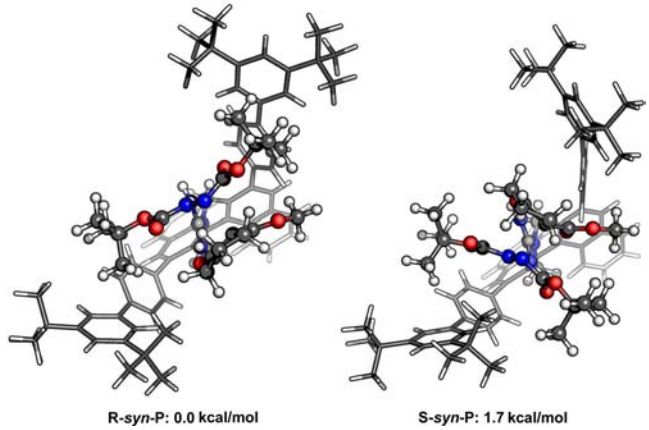

Figure 7. The two most stable transition structures for the reaction of 1,3-dicarbonyl compound **2** to di-*tert*-butyl azadicarboxylate. In the *R* transition state, nucleophile and electrophile fit in the groove defined by the 3,3′ substituents of the catalyst.

Frontal views of *syn* transition structures leading to *R* products show that the catalyst 3,3′ substituents define a groove in which the 1,3-dicarbonyl compound and the electrophile are in a parallel arrangement. These groups are distributed perpendicularly within the groove in the *syn P* guanidine transition states that lead to the *S* products. This leads to steric repulsion with the catalyst's substituents and explains its reduced stability (+1.7 kcal/mol in the best case, Figure 7). The steric repulsion is reduced when guanidine adopts the *M* conformation, but only after the guanidine is twisted, losing its planarity (the C−N−C═N dihedral angle in these transition structures over 30°). This leads to transition structures with even higher energy (4.6 kcal/mol in the best case). It is also possible to release the steric interactions in *S* transition states by rotating the reactants and placing the ester O-atom (instead of the ketone O-atom) closer to the guanidine N-atom. However, only more unstable transition structures are obtained (11.1 kcal/mol in the best case).

In previous works,[50−53] we proposed a model to explain the enantioselectivity of imine reactions catalyzed by BINOP based on a projection of the catalyst in which the two BINOP O-atoms actively involved in the catalysis are eclipsed (Figure 8a). A similar model is also useful to explain the allylboration of aldehydes catalyzed by BINOP.[81] Himo and Marcelli[54] and Gridnev and Terada[82] have also suggested that the stereochemistry of the BINOP imine reactions can be predicted on the basis of a model in which the catalyst is viewed across the C_2 symmetry axis. When trying to apply any of these models to the axially chiral guanidine catalysts, we noticed that the guanidine N-atoms occupy a different position, since the tetrahedral P-atom in BINOP and the planar guanidine arrange their substituents differently (Figure 8b).

Instead of using the models for BINOP, which are not valid in this case, we propose that the absolute configuration of the major enantiomer can be predicted by a different model. First, the catalyst is projected leaving the guanidinium on the plane of the paper; on this structure, the diazadicarboxylates are H-bonded to the guanidinium N-atoms so the protonated N-atom is in the same plane as the guanidinium. Two possible orientations of the electrophile are possible, but one leaves the biggest part of the diazadicarboxylate toward the most hindered region of the catalyst and can be discarded (Figure 8c). The enolate can then be H-bonded to the guanidinium, leaving again the O-atom in the same plane as the guanidinium atoms. There are

dx.doi.org/10.1021/ja307712y | J. Am. Chem. Soc. 2012, 134, 16869−16876

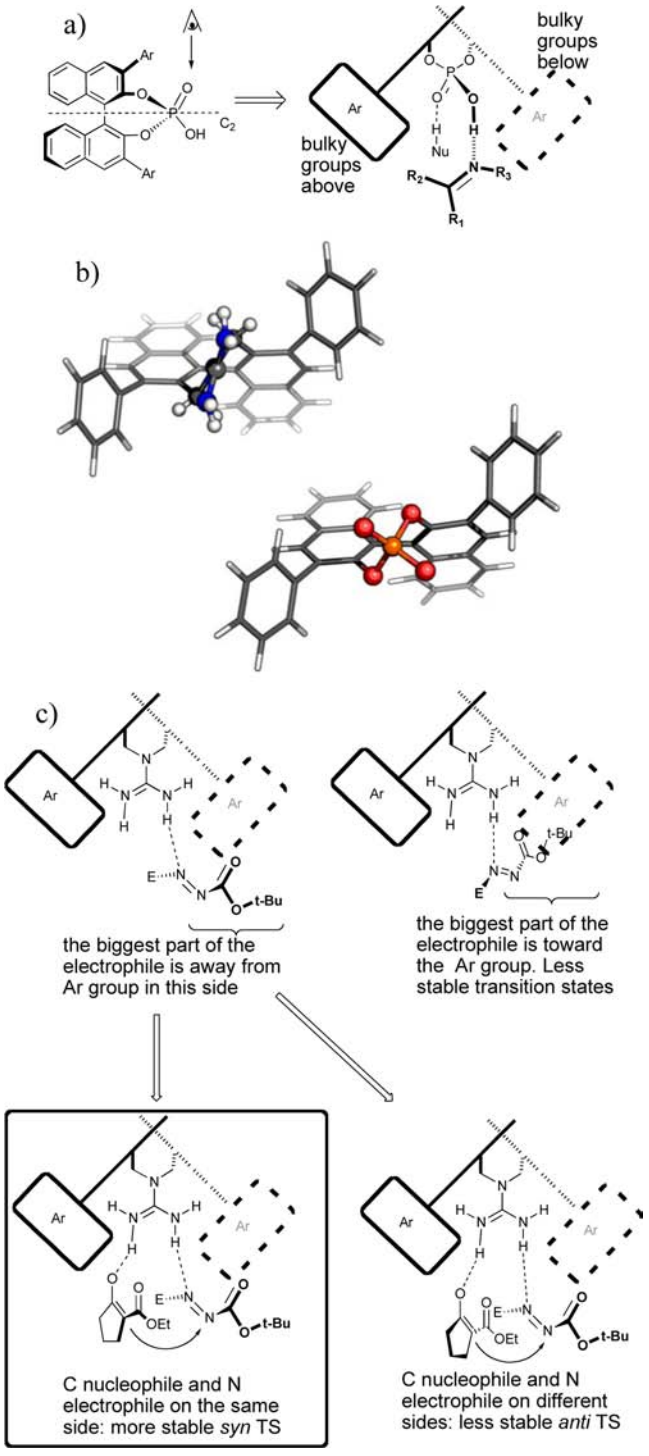

Figure 8. (a) Model to predict the stereoselectivity for the reaction of imines catalyzed by BINOP. (b) Differences in the arrangement of BINOP-active O-atoms and N-atoms in Terada's axially chiral guanidine. (c) Model to predict the enantioselectivity of the reaction catalyzed by Terada's axially chiral guanidine.

two possible orientations of the enolate, but when the reacting atoms are on different sides, *anti* (less stable) transition structures are obtained. The most stable transition state corresponds to the *syn* transition structure in which the smallest part of the electrophile is directed toward the bulky substituents in the catalyst.

Since our model explains the enantioselectivity for the reaction of β-keto ester **2**, we turned out attention the reactions of the acyclic substrate **3**, which shows a surprising reversal in selectivity. As before, we modeled the reaction for the methyl ester instead of the ethyl ester to simplify the calculations. We found transition structures analogous to those of the cyclic β-keto ester (in this case, no *anti* transition state was included, because of their high relative energy in the reaction of **2**). The results, which are summarized in Figure 8, show a similar trend, and the most stable (by 3.4 kcal/mol) transition state corresponds to *R* stereochemistry. Therefore, these calculations do not predict the enantiomeric selectivity of the reaction obtained experimentally (85% ee for *S* product).

So far, the model only considers the *Z* enolate. For the cyclic system, no other enolate is possible, but for the acyclic case, an *E* enolate can also form. The change from *Z* to *E* enolate implies that the absolute configuration on the generated quaternary center will be reversed, but the steric interactions and factors determining the relative stability of the transition structures will mainly be maintained, so the most stable *Z-syn-R* transition structures may lead to *E-anti-S* analogues. This is, indeed, the case: the most stable transition structure contains the *E* enolate and leads to the *S* product (Figure 9). When the zero-point-corrected energies are used to predict the enantioselectivity of the reaction, a 77% ee in favor of *S* product is obtained, in reasonably good agreement with experimental results. Furthermore, this also explains the different enantioselectivity for the reaction of **2** and **3** dicarbonyl compounds, since the *E* enolate is not accessible from cyclic β-keto ester **2**. Interestingly, the enantioselectivity of the reaction is slightly increased when ethyl ester in **3** is replaced by a *tert*-butyl ester (85% ee to 88% ee), because in *E* enolate transition state the ester group points away from the catalyst. However, when an ethyl instead of a methyl group is present in the α position of **3**, the enantioselectivity is reduced to 62% ee, which could be explained by considering that this alkyl group is directed toward the structure of the guanidine catalyst (see Figure 10), destabilizing the most stable transition structure.

It is surprising that the enolate adopts an *E* configuration in the most stable transition structure. The most stable configuration for the enol form of β-ketoester is *Z* since this makes possible an intramolecular H-bond between both carbonyl oxygens. Using the same level of theory used in transition-state calculations, we estimate that *Z* enol is 8.5 kcal/mol more stable. However, in the transition states of the reaction this proton has already been transferred to the guanidine. When *Z* and *E* enolate structures are compared, the former is 8.8 kcal/mol less stable than the latter, opposite to the result observed in the enol. The situation in the transition state of the reaction is probably not as extreme, since in transition structures bearing the *Z* enolate there exists the possibility of electrostatic interactions between the partial positive charge in the guanidinium and the partial negative charge in the ester oxygen, which is missed in the *E* enolate transition states. This leads to a situation in which it is possible to find competing transition states with similar energies yielding opposite enantiomers.

It is possible to find in the literature more examples in which cyclic and acyclic 1,3-dicarbonyl compounds lead to opposite enantiomers (Figure 10). In his study of the addition of 1,3-dicarbonyl compounds to nitroolefins catalyzed by an amino thiourea catalyst, Takemoto[83] also observed the formation of different epimers for the reactions of acyclic and cyclic β-keto esters (Figure 11). Independently, Wang et al.[84] observed the same effect in this reaction with a related catalyst. In the alkylation of N-Boc imines, Kim and Kang observed a considerably smaller stereoselectivity for acyclic than for

dx.doi.org/10.1021/ja307712y | J. Am. Chem. Soc. 2012, 134, 16869−16876

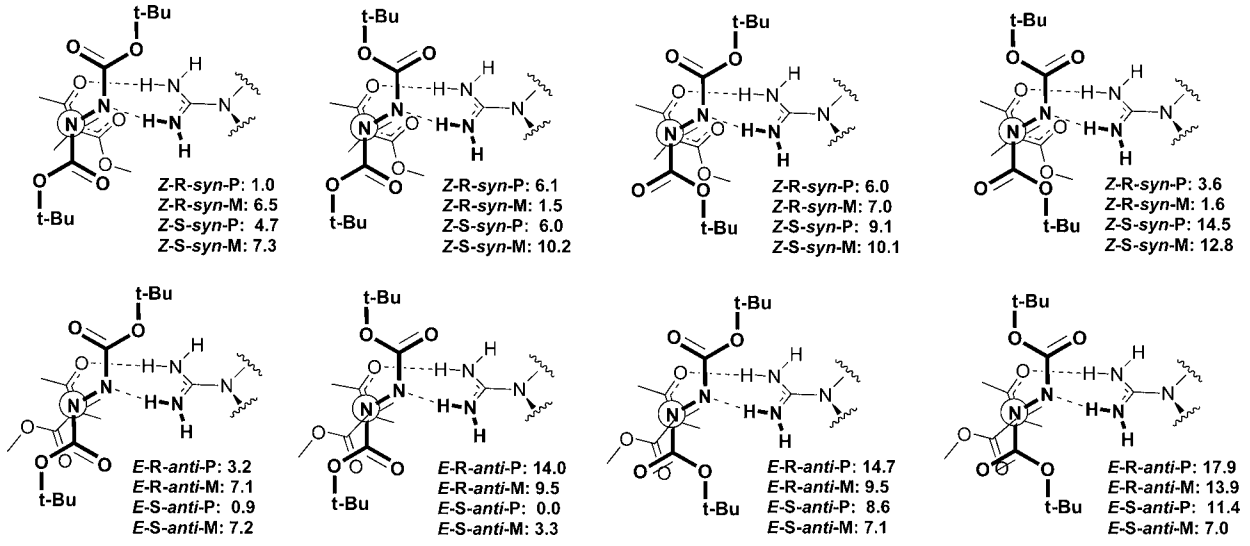

Figure 9. Transition structures for the addition of acyclic 1,3-dicarbonyl compound **3** to di-*tert*-butyl azadicarboxylate catalyzed by chiral guanidine **1**. Note that only *S* transition structures are shown. Energies relative to the most stable transition state are expressed in kcal/mol.

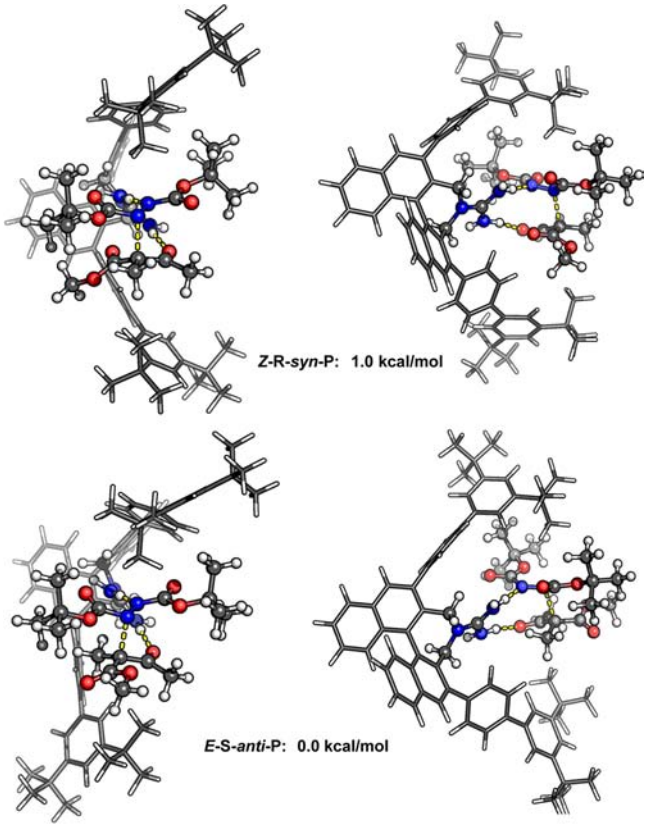

Figure 10. The two most stable transition structures for the reaction of 1,3-dicarbonyl compound **3** to di-*tert*-butyl azadicarboxylate. In both transition structures, nucleophile and electrophile fit in the groove defined by the 3,3′ substituents of the catalyst. In the *E* enolate transition state, the ester group (and not the α methyl group) points away from the catalyst structure.

cyclic cyclic β-keto esters.[85] Similar results were obtained by Yun and Kim[86] and independently by Zhang et al.[87] in a reaction similar to the one that we study here, but using an amino-thiourea organocatalyst. It is possible that competition between *E* and *Z* enolates reduces the enantioselectivity in the case of the acyclic substrates in these latter examples.

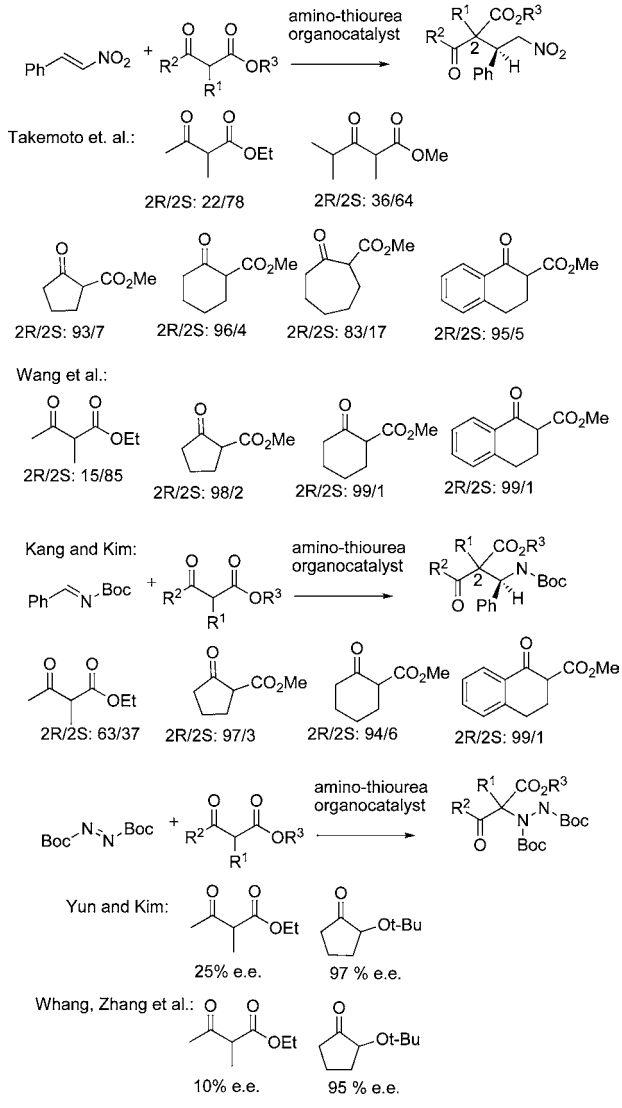

Figure 11. Several examples from the literature in which the stereochemistry of organocatalyzed reactions of β-keto esters is reversed or reduced for acyclic substrates.

dx.doi.org/10.1021/ja307712y | J. Am. Chem. Soc. 2012, 134, 16869−16876

CONCLUSIONS

The mechanism of the reaction of β-keto esters with azadicarboxylates catalyzed by an axially chiral guanidine has been investigated. Like reactions catalyzed with BINOP organocatalysts, the results are consistent with a mechanism in which the guanidine catalyst interacts simultaneously with the nucleophile and the electrophile. The stereoinduction in the reaction can be explained by means of the three-point contact model, since, in addition to the two H-bonds between the catalysts and the reactants, a third interaction (destabilizing steric hindrance) is present in the transition state leading to the minor enantiomer. In the case of cyclic β-keto esters, once the factors that contribute to the stability of the transition state are identified (as the relative orientation of the nucleophile and the electrophile), it is possible to predict the major enantiomer as the reactant distribution that fits in the cavity defined by the catalyst 3,3′ substituents.

In acyclic β-keto esters the situation is more complicated, since it is necessary to consider the possibility that the enolate adopts an *E* configuration, yielding transition structures with similar energies. To the best of our knowledge, this is the first mechanistic study that shows the acyclic β-keto esters can react through the *E* configuration, but the literature already contains several experimental results that indicate that this is feasible. We are currently performing further calculations to check if the explanation found here for the reversal in the stereochemistry for cyclic and acyclic β-ketoesters can be extended to more organocatalytic reactions.

ASSOCIATED CONTENT

Supporting Information

Complete ref 63; Cartesian coordinates of calculated structures. This material is available free of charge via the Internet at http://pubs.acs.org.

AUTHOR INFORMATION

Corresponding Author

lsimon@usal.es; jmg11@cam.ac.uk

Notes

The authors declare no competing financial interest.

ACKNOWLEDGMENTS

This research was supported by a Marie Curie Intra-European Fellowship within the sixth European Community Framework Programme MEIF-CT2006-040554 and a Marie-Curie Reintegration Grant within the seventh European Community Framework Programme PERG04-GA-2008-239244. We acknowledge the use of CamGrid service in carrying out this work.

REFERENCES

(1) Leow, D.; Tan, C.-H. *Chem.—Asian J.* **2009**, *4*, 488.
(2) Corey, E. J.; Grogan, M. J. *Org. Lett.* **1999**, *1*, 157.
(3) Ishikawa, T.; Isobe, T. *Chem.—Eur. J.* **2002**, *8*, 552.
(4) Shen, J.; Nguyen, T. T.; Goh, Y.-P.; Ye, W.; Fu, X.; Xu, J.; Tan, C.-H. *J. Am. Chem. Soc.* **2006**, *128*, 13692.
(5) Lohmeijer, B. G. G.; Dubois, G.; Leibfarth, F.; Pratt, R. C.; Nederberg, F.; Nelson, A.; Waymouth, R. M.; Wade, C.; Hedrick, J. L. *Org. Lett.* **2006**, *8*, 4683.
(6) Pratt, R. C.; Lohmeijer, B. G. G.; Long, D. A.; Waymouth, R. M.; Hedrick, J. L. *J. Am. Chem. Soc.* **2006**, *128*, 4556.
(7) Ye, W.; Jiang, Z.; Zhao, Y.; Goh, S. L. M.; Leow, D.; Soh, Y.-T.; Tan, C.-H. *Adv. Synth. Catal.* **2007**, *349*, 2454.
(8) Ghobril, C.; Sabot, C.; Mioskowski, C.; Baati, R. *Eur. J. Org. Chem.* **2008**, 4104.
(9) Leow, D.; Lin, S.; Chittimalla, S. K.; Fu, X.; Tan, C.-H. *Angew. Chem.* **2008**, *120*, 5723.
(10) Helou, M.; Miserque, O.; Brusson, J.-M.; Carpentier, J.-F.; Guillaume, S. M. *Chem.—Eur. J.* **2010**, *16*, 13805.
(11) Sohtome, Y.; Shin, B.; Horitsugi, N.; Takagi, R.; Noguchi, K.; Nagasawa, K. *Angew. Chem., Int. Ed.* **2010**, *49*, 7299.
(12) Sohtome, Y.; Tanaka, S.; Takada, K.; Yamaguchi, T.; Nagasawa, K. *Angew. Chem., Int. Ed.* **2010**, *49*, 9254.
(13) Cho, B.; Tan, C.-H.; Wong, M. W. *Org. Biomol. Chem.* **2011**, *9*, 4550.
(14) Dong, S.; Liu, X.; Zhang, Y.; Lin, L.; Feng, X. *Org. Lett.* **2011**, *13*, 5060.
(15) Appel, E. A.; Lee, V. Y.; Nguyen, T. T.; McNeil, M.; Nederberg, F.; Hedrick, J. L.; Swope, W. C.; Rice, J. E.; Miller, R. D.; Sly, J. *Chem. Commun.* **2012**, *48*, 6163.
(16) Gupta, M. K.; Li, Z.; Snowden, T. S. *J. Org. Chem.* **2012**, *77*, 4854.
(17) Li, L.; Chen, W.; Yang, W.; Pan, Y.; Liu, H.; Tan, C.-H.; Jiang, Z. *Chem. Commun.* **2012**, *48*, 5124.
(18) Wang, J.; Chen, J.; Kee, C. W.; Tan, C.-H. *Angew. Chem., Int. Ed.* **2012**, *51*, 2382.
(19) Zhao, Y.; Lim, X.; Pan, Y.; Zong, L.; Feng, W.; Tan, C.-H.; Huang, K.-W. *Chem. Commun.* **2012**, *48*, 5479.
(20) Terada, M.; Ube, H.; Yaguchi, Y. *J. Am. Chem. Soc.* **2006**, *128*, 1454.
(21) Terada, M.; Ikehara, T.; Ube, H. *J. Am. Chem. Soc.* **2007**, *129*, 14112.
(22) Ube, H.; Shimada, N.; Terada, M. *Angew. Chem., Int. Ed.* **2010**, *49*, 1858.
(23) Terada, M.; Amagai, K.; Ando, K.; Kwon, E.; Ube, H. *Chem.—Eur. J.* **2011**, *17*, 9037.
(24) Terada, M.; Ando, K. *Org. Lett.* **2011**, *13*, 2026.
(25) Terada, M.; Nii, H. *Chem.—Eur. J.* **2011**, *17*, 1760.
(26) Terada, M. *J. Synth. Org. Chem., Jpn.* **2010**, *68*, 1159.
(27) Terada, M.; Nakano, M. *Heterocycles* **2008**, *76*, 1049.
(28) Terada, M.; Fukuchi, S.; Amagai, K.; Nakano, M.; Ube, H. *ChemCatChem* **2012**, *4*, 963.
(29) Kiesewetter, M. K.; Scholten, M. D.; Kirn, N.; Weber, R. L.; Hedrick, J. L.; Waymouth, R. M. *J. Org. Chem.* **2009**, *74*, 9490.
(30) Li, J.; Jiang, W.-Y.; Han, K.-L.; He, G.-Z.; Li, C. *J. Org. Chem.* **2003**, *68*, 8786.
(31) Simon, L.; Goodman, J. M. *J. Org. Chem.* **2007**, *72*, 9656.
(32) Chuma, A.; Horn, H. W.; Swope, W. C.; Pratt, R. C.; Zhang, L.; Lohmeijer, B. G. G.; Wade, C. G.; Waymouth, R. M.; Hedrick, J. L.; Rice, J. E. *J. Am. Chem. Soc.* **2008**, *130*, 6749.
(33) Hammar, P.; Ghobril, C.; Antheaume, C.; Wagner, A.; Baati, R.; Himo, F. *J. Org. Chem.* **2010**, *75*, 4728.
(34) Fu, X.; Tan, C.-H. *Chem. Commun.* **2011**, *47*, 8210.
(35) Pan, Y.; Kee, C. W.; Jiang, Z.; Ma, T.; Zhao, Y.; Yang, Y.; Xue, H.; Tan, C.-H. *Chem.—Eur. J.* **2011**, *17*, 8363.
(36) Akiyama, T. *Chem. Rev.* **2007**, *107*, 5744.
(37) You, S.-L. *Chem.—Asian J.* **2007**, *2*, 820.
(38) Terada, M. *Chem. Commun.* **2008**, 4097.
(39) Zamfir, A.; Schenker, S.; Freund, M.; Tsogoeva, S. B. *Org. Biomol. Chem.* **2010**, *8*, 5262.
(40) Yu, J.; Shi, F.; Gong, L.-Z. *Acc. Chem. Res.* **2011**, *44*, 1156.
(41) Yu, X.; Wang, W. *Chem.—Asian J.* **2008**, *3*, 516.
(42) Rueping, M.; Kuenkel, A.; Atodiresei, I. *Chem. Soc. Rev.* **2011**, *40*, 4539.
(43) Akiyama, T.; Itoh, J.; Yokota, K.; Fuchibe, K. *Angew. Chem., Int. Ed.* **2004**, *43*, 1566.
(44) Uraguchi, D.; Sorimachi, K.; Terada, M. *J. Am. Chem. Soc.* **2004**, *126*, 11804.
(45) Uraguchi, D.; Terada, M. *J. Am. Chem. Soc.* **2004**, *126*, 5356.
(46) Terada, M.; Nakano, M.; Ube, H. *J. Am. Chem. Soc.* **2006**, *128*, 16044.
(47) Terada, M.; Tsushima, D.; Nakano, M. *Adv. Synth. Catal.* **2009**, *351*, 2817.
(48) Ube, H.; Terada, M. *Bioorg. Med. Chem. Lett.* **2009**, *19*, 3895.

(49) Nakano, M.; Terada, M. *Synlett* **2009**, *2009*, 1670.
(50) Simón, L.; Goodman, J. M. *J. Am. Chem. Soc.* **2008**, *130*, 8741.
(51) Simón, L.; Goodman, J. M. *J. Am. Chem. Soc.* **2009**, *131*, 4070.
(52) Simón, L.; Goodman, J. M. *J. Org. Chem.* **2010**, *75*, 589.
(53) Simón, L.; Goodman, J. M. *J. Org. Chem.* **2011**, *76*, 1775.
(54) Marcelli, T.; Hammar, P.; Himo, F. *Chem.—Eur. J.* **2008**, *14*, 8562.
(55) Akiyama, T.; Morita, H.; Bachu, P.; Mori, K.; Yamanaka, M.; Hirata, T. *Tetrahedron* **2009**, *65*, 4950.
(56) Marcelli, T.; Hammar, P.; Himo, F. *Adv. Synth. Catal.* **2009**, *351*, 525.
(57) Mori, K.; Katoh, T.; Suzuki, T.; Noji, T.; Yamanaka, M.; Akiyama, T. *Angew. Chem., Int. Ed.* **2009**, *48*, 9652.
(58) Shi, F.-Q.; Song, B.-A. *Org. Biomol. Chem.* **2009**, *7*, 1292.
(59) Yamanaka, M.; Hirata, T. *J. Org. Chem.* **2009**, *74*, 3266.
(60) Xu, S.; Wang, Z.; Li, Y.; Zhang, X.; Wang, H.; Ding, K. *Chem.—Eur. J.* **2010**, *16*, 3021.
(61) Zheng, C.; Sheng, Y.-F.; Li, Y.-X.; You, S.-L. *Tetrahedron* **2010**, *66*, 2875.
(62) Vadim, A. D. *Chirality* **1997**, *9*, 99.
(63) Frisch, M. J.; et al. *Gaussian 09*, Revision B.01; Gaussian, Inc.: Wallingford, CT, 2009.
(64) Svensson, M.; Humbel, S.; Morokuma, K. *J. Chem. Phys.* **1996**, *105*, 3654.
(65) Dapprich, S.; Komáromi, I.; Byun, K. S.; Morokuma, K.; Frisch, M. J. *J. Mol. Struct.* **1999**, *461*, 1.
(66) Vreven, T.; Morokuma, K. *J. Comput. Chem.* **2000**, *21*, 1419.
(67) Rappé, A. K.; Casewit, C. J.; Colwell, K. S.; Goddard, W. A., III; Skid, W. M. *J. Am. Chem. Soc.* **1992**, *114*, 10024.
(68) Becke, A. D. *J. Chem. Phys.* **1983**, *98*, 5648.
(69) Clark, T.; Chandrasekhar, J.; Schleyer, P. v. R. *J. Comput. Chem.* **1983**, *4*, 294.
(70) Gill, P. M. W.; Johnson, B. G.; Pople, J. A.; Frisch, M. J. *Chem. Phys. Lett.* **1992**, *197*, 499.
(71) Krishnan, R.; Binkley, J. S.; Seeger, R.; Pople, J. A. *J. Chem. Phys.* **1980**, *72*, 650.
(72) Cammi, R.; Mennucci, B.; Tomasi, J. *J. Phys. Chem. A* **1999**, *103*, 9100.
(73) Cammi, R.; Mennucci, B.; Tomasi, J. *J. Phys. Chem. A* **2000**, *104*, 5631.
(74) Cossi, M.; Rega, N.; Scalmani, M.; Barone, V. *J. Chem. Phys.* **2001**, *114*, 5691.
(75) Cossi, M.; Scalmani, G.; Rega, N.; Barone, V. *J. Chem. Phys.* **2002**, *117*, 43.
(76) Cossi, M.; Scalmani, G.; Rega, N.; Barone, V. *J. Comput. Chem.* **2003**, *24*, 669.
(77) Zhao, H.; Truhlar, D. G. *Theor. Chem. Acta* **2007**, *120*, 215.
(78) Zhao, Y.; Truhlar, D. G. *Acc. Chem. Res.* **2008**, *41*, 157.
(79) Simon, L.; Goodman, J. M. *Org. Biomol. Chem.* **2011**, *9*, 689.
(80) Belova, N. V.; Oberhammer, H.; Girichev, G. V. *J. Phys. Chem. A* **2004**, *108*, 3593.
(81) Grayson, M. N.; Pellegrinet, S. C.; Goodman, J. M. *J. Am. Chem. Soc.* **2012**, *134*, 2716.
(82) Gridnev, I. D.; Kouchi, M.; Sorimachi, K.; Terada, M. *Tetrahedron Lett.* **2007**, *48*, 497.
(83) Okino, T.; Hoashi, Y.; Furukawa, T.; Xu, X.; Takemoto, Y. *J. Am. Chem. Soc.* **2005**, *127*, 119.
(84) Zhang, Z.-H.; Dong, X.-Q.; Chen, D.; Wang, C.-J. *Chem.—Eur. J.* **2008**, *14*, 8780.
(85) Kang, Y. K.; Kim, D. Y. *J. Org. Chem.* **2009**, *74*, 5734.
(86) Jung, S. H.; Kim, D. Y. *Tetrahedron Lett.* **2008**, *49*, 5527.
(87) Zhang, Z.-H.; Dong, X.-Q.; Tao, H.-Y.; Wang, C.-J. *ARKIVOC* **2011**, *(ii)*, 137.